Proceedings of the ASME 2016 14th International Conference on Nanochannels, Microchannels, and Minichannels
ICNMM2016
July 10-14, 2016, Washington, DC, USA

ICNMM2016-8052

ULTRATHIN SILICON MEMBRANES FOR IMPROVING EXTRACORPOREAL BLOOD THERAPIES

Tucker Burgin
Department of Biomedical Engineering
University of Rochester, 252 Elmwood Ave Rochester, NY 14627
(303) 552-6861, tburgin@ur.rochester.edu

Dean Johnson[1], **Henry Chung**[1], **Alfred Clark, Jr.**[2], **James McGrath**[1]
[1]: Department of Biomedical Engineering
[2]: Department of Mechanical Engineering
University of Rochester, 252 Elmwood Ave Rochester, NY 14627

ABSTRACT

Extracorporeal blood therapies such as hemodialysis and extracorporeal membrane oxygenation supplement or replace organ function by the exchange of molecules between blood and another fluid across a semi-permeable membrane. Traditionally, these membranes are made of polymers with large surface areas and thicknesses on the scale of microns. Therapeutic gas exchange or toxin clearance in these devices occurs predominantly by diffusion, a process that is described by an inverse square law relating a distance to the average time a diffusing particle requires to travel that distance. As such, small changes in membrane thickness or other device dimensions can have significant effects on device performance – and large changes can cause dramatic paradigm shifts. In this work, we discuss the application of ultrathin nanoporous silicon membranes (nanomembranes) with thicknesses on the scale of tens of nanometers to diffusion-mediated medical devices. We discuss the theoretical consequences of nanomembrane medical devices for patients, analyzing several notable benefits such as reduced device size (enabling wearability, for instance) and improved clearance specificity. Special attention is paid to computational and analytical models that describe real experimental behavior, and that in doing so provide insights into the relevant parameters governing the devices.

INTRODUCTION

Extracorporeal blood therapies such a hemodialysis and extracorporeal membrane oxygenation (ECMO) have seen little innovation over the last several decades despite poor outcomes for patients reliant on these technologies. These treatments involve transport of solutes into or out of blood through a semi-permeable membrane in an extracorporeal blood circuit. The membranes employed for these processes are typically regenerated cellulose or synthetic polymer, and are many microns in thickness. To compensate for their poor permeabilities membranes with very large areas are employed, typically arrayed into a bundle of hollow fibers to maximize transport.

Due to their large membrane areas (and thus high hydraulic resistances) these devices are made very large to accommodate not only the large fiber bundles, but a significant volume of tubing, a pumping apparatus, and other elements. This may be problematic depending on the application. For instance, in hemodialysis the size of dialysis devices restricts the availability of the treatment to patients to short and somewhat infrequent sessions, in effect denying them access to the life-sustaining functions of renal replacement therapy. The deleterious effect of this infrequency in treatment is apparent in the fact that dialysis patients are most likely to suffer hospitalization and death on the days just before their scheduled treatments [1, 2], and that more frequent treatments are associated with improved patient outcome [3, 4].

Similarly, while ECMO devices are for intensive care applications and thus may be immobile without limiting the patient's access, the large extracorporeal blood volume can be itself extremely dangerous due (for instance) to the need for frequent red blood cell transfusions, which have been shown to be an independent risk factor in patient morbidity and mortality [5]. This is especially true in pediatric and neonatal patients, for whom the extracorporeal circuit volume could be as much as twice their own blood volume [6]. Furthermore, for the cardiac health of the patient (and especially children) extracorporeal circuits representing more than roughly 10% of the patient's blood volume are considered undesirable [7].

The large device sizes and extracorporeal blood volumes of current dialysis and ECMO devices are direct products of the active membrane area required for these devices to allow for adequate blood solute transport to occur. Our contention is that increasing the transport efficiency of the membranes used in these applications would enable a reduction in device size, which in turn would have direct positive effects on patient health.

In order to arrive at this increased efficiency, we pro-

pose the application of ultrathin silicon membranes to these therapies. Initially reported in pure crystalline silicon by Striemer et al., this class of highly permeable materials is molecularly thin and yet mechanically robust [8]. By reducing the diffusion distance of solutes across the membrane by two to three orders of magnitude compared to traditional membranes, the average diffusion time is reduced by ten-thousand to a million times, affecting a massive increase in the efficiency of transmembrane diffusion.

In this work, we present a theoretical framework for modeling the relevant transport problems in these sorts of devices. We develop analytical and computational models and demonstrate their effectiveness in predicting the results of experiments. In this way we demonstrate the promising possibilities represented by nanomembrane-enabled miniaturized hemotherapeutic devices and pave the way for future prototyping and testing towards making them a reality.

METHODS AND MODELS

Silicon Nanomembranes

The highly porous, exceedingly thin, and strikingly robust pure silicon nanomembranes developed by Striemer et al. [8] are an ideal material for extracorporeal blood therapies. A recent publication by our group describes a further improvement in this technology with the creation of silicon nitride membranes, which are significantly stronger and more chemically inert [9]. The materials can be tuned for a desirable average pore size and thickness in order to maximize their applicability to a given device.

These membranes have been shown to act as walls to convective flow (that is, flows on either side of the membrane do not couple to one another [10]). In diffusion, they behave as anisotropic, non-absorbing spaces in which the effective diffusion coefficient can be calculated using the scheme described by Dechadilok and Deen [11, 12].

Hemodialysis

Experimental System The experimental system that our models attempt to predict the behavior of consists of two channels separated by a 300 micrometer-thick chip supporting a 2-by-0.7 millimeter nanoporous silicon nitride nanomembrane. 1X phosphate buffered saline (pH 7.4) is employed in both the dialysate and the blood channels, and the latter is spiked with a known concentration of an analyte before the experiment begins.

A photograph of the system is shown in Figure 1. The dialysate channel is 2 millimeters wide and 300 micrometers tall, while the blood channel is 1 millimeter wide and has a variable height (100, 300, or 1000 micrometers). The flow rate in the dialysate channel was 9 cubic millimeters per second, and varied in the blood channel depending on the channel height (0.02, 0.06, or 0.2 cubic millimeters per second) to obtain an average velocity of 0.2 millimeters per second.

The results of each experiment were obtained by assaying the fluid at the blood channel outlet for the appropriate analyte. Three analytes and three assays were used: urea (BioVision Urea Colorimetric Assay Kit, catalog #K375-100), cytochrome c (absorbance at 410 nanometers), and bovine serum albumin (ThermoFisher Scientific Quant-iT Protein Assay, catalog #Q33210).

Analytical Model The transport of blood solutes in hemodialysis is governed by the convection-diffusion equation:

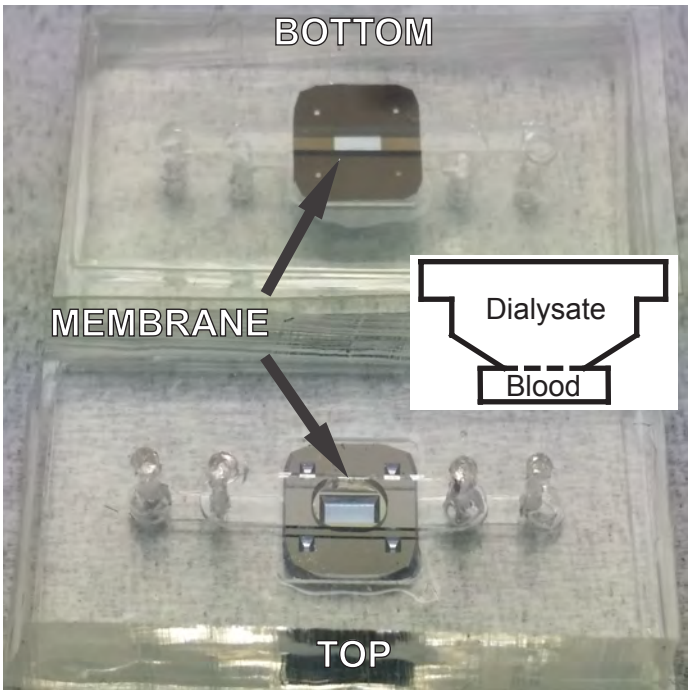

FIGURE 1: A photograph of two experimental systems, one inverted to show the bottom. The blood channel inlets and outlets are the outermost holes and the channel passes under the membrane, while the dialysate channel inlets and outlets are the innermost holes and the channel passes over the top. The 2-by-0.7 millimeter membrane is indicated. Inset: An idealized cross section of the device at the membrane, which is marked by a dashed line. The height of the blood channel is variable.

$$\frac{\partial c}{\partial t} = D_0 \nabla^2 c + v \nabla c \tag{1}$$

where the first term on the right side is diffusion governed by the solute diffusivity D_0 and the second is convection governed by the velocity field v.

To arrive at a preliminary analytical solution, we made three simplifying assumptions. First, we approximated the velocity field as constant within the channel. We also assume that diffusion is negligible in the direction of flow and that the concentration in the dialysate is negligible at all times. With these assumptions in place, we can non-dimensionalize the problem:

$$\frac{\partial \bar{c}}{\partial \bar{t}} = \frac{\partial^2 \bar{c}}{\partial \bar{x}^2} \tag{2}$$

for $0 \leq \bar{x} < 1$ and $\bar{t} \geq 0$, where

$$\bar{x} = \frac{x}{a};\ \bar{c} = \frac{c}{c_0};\ \bar{t} = \frac{t D_0}{a^2} \tag{3}$$

and where we can see that defining dimensional time t as the length of the membrane divided by v eliminates the concentration profile's dependance on the two spatial dimensions

in which diffusion does not occur. Here, a is the distance from membrane to wall in the blood channel, and c_0 is the initial concentration of the diffusing solute.

We can define the resistance of the membrane to transmembrane diffusion of solutes as a fraction of the overall resistance to transport in that direction via a new term:

$$\beta = \frac{d/D_m}{a/D_0} \tag{4}$$

Here, the ratio of membrane thickness d to solute diffusivity within the membrane D_m is compared to the same ratio for the fluid space. Incorporating this term, the boundary conditions for this problem are:

$$\frac{\partial \bar{c}}{\partial \bar{x}}(0,\bar{t}) = 0 \tag{5}$$

$$\bar{c}(\bar{x},0) = 1 \tag{6}$$

$$\bar{c}(1,\bar{t}) + \beta \frac{\partial \bar{c}}{\partial \bar{x}}(1,\bar{t}) = 0 \tag{7}$$

In the case that β is negligible, the solution to this problem is [12]:

$$\bar{c}(\bar{x},\bar{t}) = \frac{2}{\pi} \sum_{n=1}^{\infty} \frac{(-1)^{n+1}}{n - {}^1\!/_2} cos(\pi(n - {}^1\!/_2)\bar{x}) e^{-(\pi(n-{}^1\!/_2))^2 \bar{t}} \tag{8}$$

Otherwise, it is:

$$\bar{c}(\bar{x},\bar{t}) = \sum_{n=1}^{\infty} \frac{2sin(z_n)cos(z_n\bar{x})}{z_n + sin(z_n)cos(z_n)} e^{-z_n^2\bar{t}} \tag{9}$$

The values of z_n in Equation 9 are obtained by finding the solutions to an eigenfunction:

$$tan(z_n) = \frac{1}{\beta z_n} \tag{10}$$

where z_1 is the smallest solution, and so on. Fractional clearance from the device can be obtained by subtracting from one the average value of the concentration profile calculated at the outlet. This model can be corrected somewhat to account for less than 100% active membrane area by scaling its output by the active area fraction, but this is only an empirical improvement.

Computational Model Under certain conditions of complicated dialyzer geometry or when the assumptions made by the analytical model are not suitable, a computational approach enables us to continue to make accurate predictions of system behavior at the cost of speed. We built our computational models using the COMSOL Multiphysics 4.2a software package across three computational domains and two types of physics simulations.

The computation is split into the distinct domains of the blood channel, the dialysate channel, and the membrane. The former two contain simulations of both Navier-Stokes laminar fluid flow and Fickian diffusion, while the latter contains diffusion only. The model is first solved for flow fields in both fluid domains, and these are passed as convective terms to the diffusion simulation. The steady-state outlet concentration as a fraction of the inlet concentration in the blood channel is taken to be the fractional clearance of the solute from the dialyzer.

Model Validation The models were validated by comparison to experiments across a range of blood channel heights and experimental analytes (each with a different diffusion coefficient). The results of these comparisons are shown in Figure 2. The models were good predictors of experimental outcomes, especially the computational model (presumably due to its reduced reliance on simplifying assumptions compared to the analytical model).

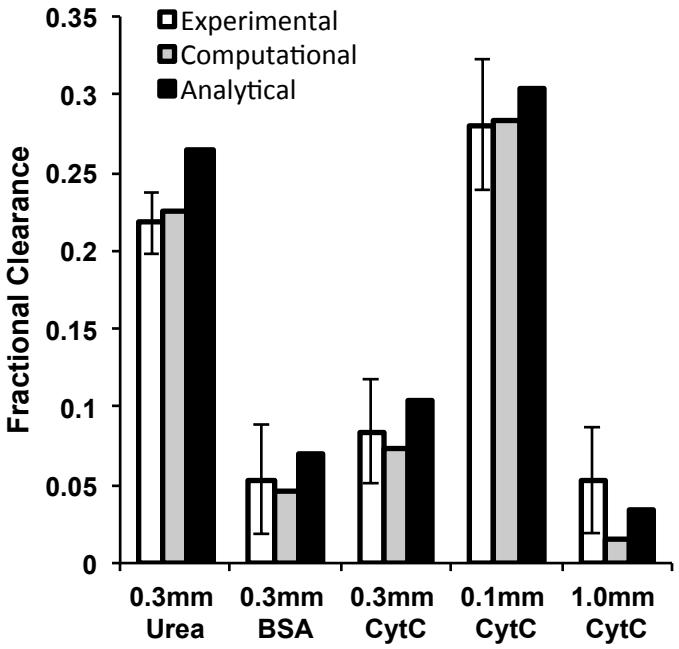

FIGURE 2: Comparison between the analytical and computational models under varying blood channel heights and analyte diffusivities, and the corresponding experimental results. Analytes were urea (approximate molecular weight 60 Da), bovine serum albumin (BSA, MW 66.5 kDa), and cytochrome c (CytC, MW 12 kDa). Error bars represent standard error of the mean at n = 3 to 4. The models were generally quite predictive of experiments, though the analytical model was typically less accurate due to its several simplifying assumptions.

Extracorporeal Membrane Oxygenation

Similarly to hemodialysis, oxygenation in ECMO can be described analytically through partial differential equations. However, in this case three simultaneous equations are required – one for oxygen, one for deoxyhemoglobin, and one for oxygenated hemoglobin – and an additional term must be included for the reaction between the species [13].

$$\frac{\partial c_O}{\partial t} = D_O \nabla^2 c_O + v \nabla c_O - \Gamma \tag{11}$$

$$\frac{\partial c_{Hb}}{\partial t} = D_{Hb} \nabla^2 c_{Hb} + v \nabla c_{Hb} - \Gamma \tag{12}$$

$$\frac{\partial c_{HbO}}{\partial t} = D_{Hb} \nabla^2 c_{HbO} + v \nabla c_{HbO} + \Gamma \tag{13}$$

The first of these equations describes the concentration distribution of oxygen c_O while the second and third describe the distribution of hemoglobin (or more specifically, heme binding sites), both oxygen-bound c_{HbO} and unbound c_{Hb}. The diffusivity D_O is that of oxygen in blood, while D_{Hb} is the diffusivity of hemoglobin within red blood cells, which is approximately one sixth that of its free diffusivity and is assumed to be constant across all oxygenation states [14].

The reaction term is given by the expression [13]:

$$\Gamma = k \cdot c_T[(1 - S)C^{2.65} - S] \tag{14}$$

where k is the dissociation rate between heme and oxygen, c_T is the total concentration of heme, S is the oxygen saturation fraction and C is the oxygen concentration normalized to the concentration at reaction equilibrium at $S = 0.5$, c_{50}. The parameter values used here are [13]:

$$k = 44 \, \frac{1}{s} \tag{15}$$

$$c_T = 2.03 \times 10^{-5} \, \frac{mol}{mL} \tag{16}$$

$$c_{50} = 4.12 \times 10^{-8} \, \frac{mol}{mL} \tag{17}$$

Because Equations 11 through 13 are too difficult to solve analytically, we modeled the process numerically with a COMSOL model incorporating fluid flow, diffusion, and reaction. As before, the fluid flow is solved first to arrive at a velocity distribution that is passed to the diffusive (and now, reactive) model as a convective term.

The flux of gasses across semi-permeable membranes from a gaseous to a liquid phase depends inversely upon the membrane thickness, so oxygen should be expected to enter the blood through a nanomembrane 100 to 1000 times faster than through traditional ECMO membranes. Hoganson et al. [15] have reported approximately 89.3 $mL \cdot min^{-1} \cdot m^{-2}$ of oxygen flux through their 15 μm-thick membrane, suggesting that the expected flux for a nanomembrane under the same conditions should be on the order of 90,000 $mL \cdot min^{-1} \cdot m^{-2}$.

However, in order for the diffusive flux of oxygen away from the membrane towards the bulk blood to equal this rate of transport through the membrane, the concentration gradient of oxygen in the blood would have to be roughly 6 $mM \cdot \mu m^{-1}$. Since the solubility of oxygen in blood at the typical gas pressures used in ECMO is only about 1 mM, the necessary gradient would have to be maintained over the entire duration of the oxygenation process at a difference of the maximum concentration to zero oxygen over just one sixth of a micrometer, or about 167 nanometers. Since this is clearly unrealistic, the appropriate boundary condition for the oxygen at the membrane is a concentration condition of c_O equal to the solubility of oxygen in blood, rather than a flux condition.

DISCUSSION

Our models find their applications as tools in the design and prototyping of real devices for nanomembrane extracorporeal blood therapies. While much work remains to be done on the application of these tools, it is not difficult to use them in proposing proof-of-concept designs that illustrate and gauge the potential these therapies represent.

Hemodialysis

For example, consider the process of designing a miniaturized hemodialyzer. In order to maintain a given toxin's serum concentration at a certain level during a continuous hemodialysis treatment, we must clear it at a rate equal to the rate at which it is generated within the patient's body divided by that desired concentration.

$$Q \cdot f = G/C \tag{18}$$

That is, the rate at which the blood passes through the dialyzer Q multiplied by the fraction of the toxin that is cleared from the blood in a single pass f is equal to the rate at which the toxin is produced in the body G divided by the steady-state serum concentration C. This allows us to control the toxin concentration by designing a dialyzer with the appropriate flow rate and fractional clearance.

If we choose to fix the concentration of (for example) urea in the patient's blood to a reasonable value (something close to the physiological value in healthy individuals), then we must establish a relationship between the blood channel residence time t and the blood channel height a (both of which affect the values of both Q and f) that satisfies Equation 18 for the appropriate values of G and C.

We can arrive at this relationship using Equation 8, since urea is a very small molecule and as such will have a very small value of β. Estimating the rate of urea production to be 10 $mmol \cdot hr^{-1}$ [16] and choosing a target steady-state concentration of 4.6 mM, the required relationship between t and a is:

$$t = 1.55 \times 10^{-4} \, \frac{min}{mm} \cdot a + 2.47 \times 10^{-5} \, min \tag{19}$$

When this equation is satisfied, the concentration of urea in the patient's blood will always tend towards the desired value. An additional constraint can then be placed upon the system by considering a large molecule – for example, albumin – that will have a significantly large value of β. This molecule's clearance must be controlled in the same way (since many toxins bind to albumin and must be cleared along with it [17]) but this time by constraining the pore size of the membrane. Equation 9 is appropriate here. Once the relationships between residence time, pore size, and channel height have been fixed, the final design can be selected by maximizing clearance of middle molecules, such as β_2-microglobulin.

By following this process and implementing the results in the computational model to incorporate practical device

geometry, we can arrive at a design that in theory boasts superior clearance of molecules across a huge range of molecular weights and rates of generation when compared to traditional therapies, as shown in Figure 3. Perhaps not immediately apparent from the figure is that improved albumin clearance is in fact desirable over traditional treatments, which often fail to clear sufficient albumin [17].

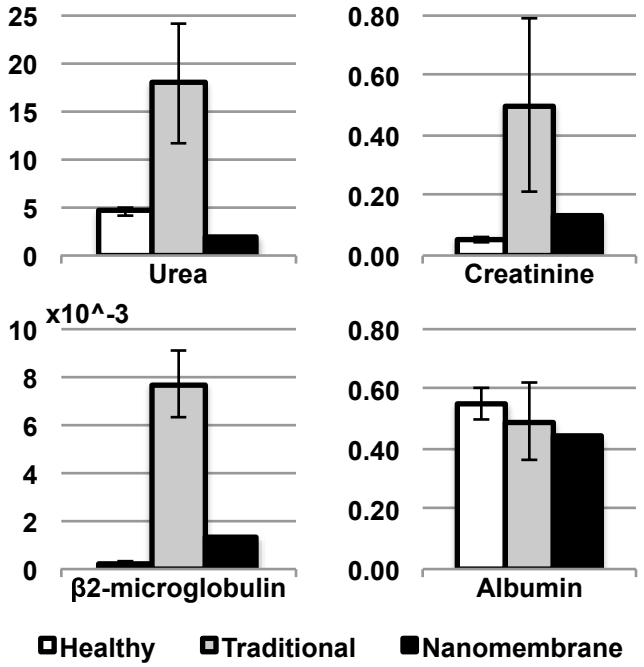

FIGURE 3: Comparison between expected serum concentrations of various uremic toxins in people with healthy renal function, people on traditional hemodialysis, and people treated with a theoretical continuous nanomembrane dialyzer. All values are millimolar. Experimental data for the Healthy and Traditional cases are reported by Mumtaz et al. [18].

Extracorporeal Membrane Oxygenation

As for the ECMO model, a total transmembrane oxygen flux for a small representative model can be measured in order to arrive at the minimum total membrane area required for complete oxygenation. The flux depends somewhat on the flow rate in the system, so the inlet flow was set to the full cardiac output of a neonatal patient (approximately 1.3 $L \cdot min^{-1}$ on the high end [19]) with 60% initial saturation.

The flux was on the order of 430 $mL \cdot min^{-1} \cdot m^{-2}$. Because at this flow rate and inlet saturation approximately 220 $mL \cdot min^{-1}$ of oxygen is required to fully saturate the blood, it is predicted that roughly 0.5 m^2 of membrane area would be required at minimum. Fashioned into a hollow fiber dialyzer with inner diameter 100 μm, the total device volume would be about 25 mL, which is very close to one tenth of a neonate's intrinsic blood volume (recall that this was the target device volume).

While this is theoretically a significant (though not revolutionary) improvement over traditional ECMO devices, achieving nanomembranes with these surface areas remains impractical for the near future. Current feasible nanomembrane areas are closer to square inches than square meters. However, future development of the technology may see nanomembrane ECMO devices become practical, in which case they might very well become the preferred treatment modality for pediatric patients with very low intrinsic blood volume.

CONCLUSION

Models of solute transport in nano-scale silicon membrane hemodialysis and ECMO have been created and used as the foundations for design and discussion of these hypothetical devices. Nanomembrane ECMO devices have been shown to be hypothetically superior to traditional devices by a small margin, assuming continued progress in the fabrication of nanomembranes with larger areas. In contrast, nanomembrane hemodialyzers are predicted to be extremely effective treatment tools with membrane areas and channel geometries already demonstrated to be possible in the laboratory. This work will continue to develop towards an experimental validation of the efficacy of nanomembrane dialysis for treatment of kidney failure.

BIBLIOGRAPHY

[1] Bleyer, A. J., Russell, G. B., and Satko, S. G., 1999. "Sudden and Cardiac Death Rates in Hemodialysis Patients". *Kidney International,* ***55***(4), pp. 1553–9.

[2] Foley, R. N., Gilbertson, D. T., Murray, T., and Collins, A. J., 2011. "Long Interdialytic Interval and Mortality Among Patients Receiving Hemodialysis". *The New England Journal of Medicine,* ***365***(12), pp. 1099–107.

[3] F. H. N. Trial Group, Chertow, G. M., Levin, N. W., Beck, G. J., Depner, T. A., Eggers, P. W., Gassman, J. J., Gorodetskaya, I., Greene, T., James, S., Larive, B., Lindsay, R. M., Mehta, R. L., Miller, B., Ornt, D. B., Rajagopalan, S., Rastogi, A., Rocco, M. V., Schiller, B., Sergeyeva, O., Schulman, G., Ting, G. O., Unruh, M. L., Star, R. A., and Kliger, A. S., 2010. "In-Center Hemodialysis Six Times per Week Versus Three Times per Week". *The New England Journal of Medicine,* ***363***(24), pp. 2287–300.

[4] Weinhandl, E. D., Liu, J., Gilbertson, D. T., Arneson, T. J., and Collins, A. J., 2012. "Survival in Daily Home Hemodialysis and Matched Thrice-Weekly In-Center Hemodialysis Patients". *Journal of the American Society of Nephrology,* ***23***(5), pp. 895–904.

[5] Smith, A. H., Hardison, D. C., Bridges, B. C., and Pietsch, J. B., 2012. "Red Blood Cell Transfusion Volume and Mortality among Patients Receiving Extracorporeal Membrane Oxygenation". *Perfusion,* ***28***(1), pp. 54–60.

[6] Friedman, D. F., and Montenegro, L. M., 2004. *Handbook of Pediatric Transfusion Medicine Chapter 17: Extracorporeal Membrane Oxygenation and Cardiopulmonary Bypass*. Hillyer, C., Strauss, R., Luban, N., eds. Elsevier Academic Press, San Diego, CA, pp. 181–9.

[7] Fischbach, M., Edefonti, A., Schrder, C., Watson, A., and The European Dialysis Working Group, 2005. "Hemodialysis in Children: General Practical Guidelines". *Pediatric Nephrology,* ***20***(8), pp. 1054–66.

[8] Striemer, C. C., Gaborski, T. R., McGrath, J. L., and Fauchet, P. M., 2007. "Charge- and Size-Based Separation of Macromolecules Using Ultrathin Silicon Membranes". *Nature,* ***445***(7129), pp. 749–53.

[9] DesOrmeaux, J., Winans, J., Wayson, S., Gaborski, T., Khire, T., Striemer, C., and McGrath, J., 2014. "Nanoporous Silicon Nitride Membranes Fabricated from Porous Nanocrystalline Silicon Templates". *Nanoscale,* ***6***(18), pp. 10798–805.

[10] Chung, H., Chan, C., Khire, T., Marsh, G., Clark, A. J., Waugh, R., and McGrath, J., 2014. "Highly Permeable Silicon Membranes for Shear Free Chemotaxis and Rapid Cell Labeling". *Lab on a Chip,* ***14***(14), pp. 2456–68.

[11] Dechadilok, P., and Deen, W. M., 2006. "Hindrance Factors for Diffusion and Convection in Pores". *Industrial & Engineering Chemistry Research,* ***45***(21), pp. 6953–9.

[12] Snyder, J., Clark, A. J., Fang, D., Gaborski, T., Striemer, C., Fauchet, P., and McGrath, J., 2011. "An Experimental and Theoretical Analysis of Molecular Separations by Diffusion through Ultrathin Nanoporous Membranes". *Journal of Membrane Science,* ***369***(1-2), pp. 119–29.

[13] Clark, A. J., Federspiel, W. J., Clark, P. A. A., and Cokelet, G. R., 1985. "Oxygen Delivery from Red Cells". *Biophysical Journal,* ***47***, pp. 171–81.

[14] Doster, W., and Longeville, S., 2007. "Microscopic Diffusion and Hydrodynamic Interactions of Hemoglobin in Red Blood Cells". *Biophysical Journal,* ***93***(4), pp. 1360–8.

[15] Hoganson, D. M., Anderson, J. L., Weinberg, E. F., Swart, E. J., Orrick, B. K., Borenstein, J. T., and Vacanti, J. P., 2010. "Branched Vascular Network Architecture: A New Approach to Lung Assist Device Technology". *The Journal of Thoracic and Cardiovascular Surgery,* ***140***(5), pp. 990–5.

[16] Lopot, F., Kotyk, P., Blha, J., and Vlek, A., 1995. "Analysis of the Urea Generation Rate and the Protein Catabolic Rate in Hemodialyzed Patients". *Artificial Organs,* ***19***(8), pp. 832–6.

[17] Liabeuf, S., Drueke, T. B., and Massy, Z. A., 2011. "Protein-Bound Uremic Toxins: New Insight from Clinical Studies". *Toxins,* ***3***(7), pp. 911–9.

[18] Mumtaz, A., Anees, M., Bilal, M., and Ibrahim, M., 2010. "Beta-2 Microglobulin Levels in Hemodialysis Patients". *Saudi Journal of Kidney Diseases and Transplantation,* ***21***(4), pp. 701–6.

[19] Hirsimaki, H., Kero, P., Wanne, O., Erkkola, R., and Makoi, Z., 1988. "Doppler-Derived Cardiac Output in Healthy Newborn Infants in Relation to Physiological Patency of the Ductus Arteriosus". *Pediatric Cardiology,* ***9***, pp. 79–83.